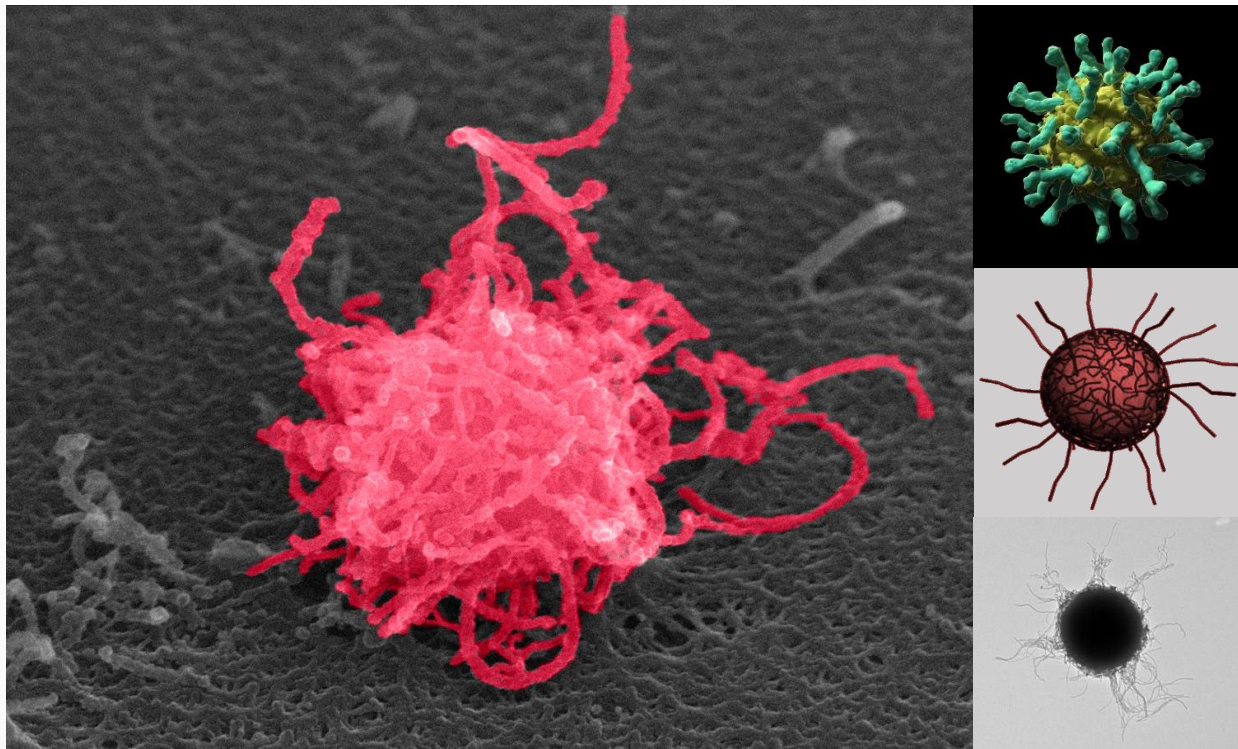


TRABAJO FIN DE MÁSTER

Carbon nanotube coated particles (CCP) for cytoplasmic delivery system



Nerea Iturrioz Rodríguez

Tutora: Mónica López Fanarraga

Junio 2016

Index

1. Introduction	3-7
1.1. Abstract	4
1.2. Introduction	5-7
2. Objectives	8-9
3. Material and Methods	10-15
3.1. HeLa cell culture	11
3.2. Particles	11
3.3. Functionalization of the particles	12
3.4. Toxicity	12
3.5. Cellular uptake	12
3.6. Staining and confocal microscopy imaging	12-13
3.7. Quantification of the particles	14
3.8. Statistical analysis	15
4. Results	16-26
4.1. CCP do not trigger cytotoxic effect	17
4.2. CNT enhance CCP entry	17-20
4.3. Control particles are exocytosed	20-24
4.4. CCP escape endo-lysosomal compartment	25-26
4.5. CCP release molecules	26
5. Discussion	27-30
6. Conclusion	31-32
7. Bibliography	32-35

1. Introduction

ABSTRACT

During years, different delivery strategies have been used such as viral and non-viral or synthetic vectors. The viral vectors have the advantage that can do a specific receptor-mediated endocytosis and escape lysosomes once are inside cells. But they can cause an immune response, provoke insertional mutagenesis and cannot deliver therapeutic proteins. Synthetic vector such as exosomes or lysosomes, don't cause immune response and can introduce proteins, but their entry mechanism is no so specific and the efficiency to integrate the cargo is lower. In the view of this, we have investigated the biosynthetic interaction of a new **carbon nanotube-coated particle** (CCP) for cytoplasmic cargo delivery. We reproduce the morphology of the typical eukaryotic viruses, often round shapes displaying spicules on their surface that serve as ligands for receptor mediated endocytosis and have designed a proof-of-concept structures that consist on a 500 nm silica sphere –future multi-purpose delivery capsules covered with carbon nanotubes to imitate the morphology of the viral spicules. Since the carbon nanotube surface is very high ($1\text{ gr}=1200\text{m}^2$) and it is highly reactive, this nanotube shell offers countless possibilities, including customization with many different ligands or proteins to interact with specific cell surface receptors. As a control we used uncoated silica spheres. This study demonstrates with flow cytometry and Trypan blue assays that the CCPs do not trigger a cytotoxic effect. Using confocal microscopy and cell live observation we show that CCPs display entry mechanisms that imitate viral particle entry (viral surfing). Moreover, transmission electron microscopy, cell live observation and confocal microscopy demonstrate how CCPs are able to escape from the endo-lysosomal membranes once they are internalized inside cells, while the uncoated control particles turn out to be exocytosed. Experiments to see the release of a colorant (5-TAMRA) attached to the carbon nanotubes, show how this particle could be useful delivering different therapy or drugs.

The current challenges in drug and gene therapy lie in the treatment of diseases such as β -thalassaemia, cancer, adenosine deaminase deficiency (ADA deficiency, ADA-SCID) among others, that are associated with problems of normal human biochemical pathways in certain tissues.

During years, scientists have been developing different strategies based on **carrier systems** to target this type of diseases (figure 1I). On the one hand, **non-viral carriers**, such as exosomes and liposomes, among others, enter into cells by membrane fusion (no-specific system) and although they are not recognised by the immune system, their efficiency of transfecting host cells is relatively low. **Viral vectors**, on the contrary, have the ability to perform specific receptor mediated endocytosis and also, once they are inside cells, are able to escape the lysosomes, delivering their genetic load into the cytoplasm. However, they can trigger an immune response (Zachary C. Hartman, Daniel M. Appledorn, 2008)), provoke an insertional mutagenesis and can only deliver nucleic acids (Seow & Wood, 2009) but not proteins or drugs. Dendrimers, highly branched spherical polymers, condense DNA via electrostatic interactions of their terminal primary amines with the DNA phosphate groups. The size, surface charge and gene transfer efficiency of dendrimer/plasmid complexes can be changed by the dendrimer concentration in the complexes (Kukowska-Latallo *et al*, 1996). After they enter cells via endocytosis, they are able to release the DNA after a swelling of the endosome due to protonation (Tang *et al*, 1996). The problem of these carriers, as with the viral vectors, is the immunogenicity they cause.

Recent advances in gene editing technologies urge the development of **new targeted delivery systems** that **can carry *ad hoc* combinations of protein and DNA**. Thus, the ideal delivery vehicle needs: i) to have an appropriate packaging size for its cargo, ii) to escape the immune system, iii) to have the highest specificity for the target cell, and iv) to efficiently deliver cargo.

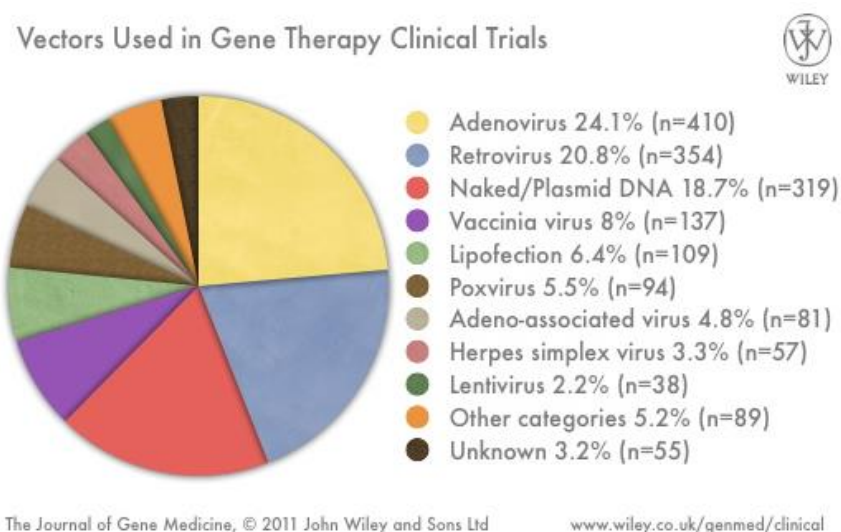


Figure 1I. Diagram showing the percentage of vector used in gene therapy clinical trials worldwide in 2011, taken from: <http://www.wiley.com/legacy/wileychi/genmed/clinical/>

Size of the carrier

It is important to have a vehicle able to transport the cargo no matter which is its size. Recent advances in gene editing technologies such as CRISPR-Cas9, need systems that can carry combinations of proteins and DNA to eukaryotic cells for editing and repair. Although the cargo size of non-viral vectors such as liposomes is variable and can be larger than the viral ones, it is necessary to bear in mind that the size of the particle can change the enter mechanism and decrease their efficiency (Canton and Battaglia, 2012).

Hide from the immune system

Another feature to take into account is the ability that the vehicle has to evade the immune system. It is known that viral vectors can provoke a stronger immune response (Zachary C. Hartman, Daniel M. Appledorn, 2008), that can be related to innate immunity, or adaptive immunity (including memory and pre-existing immunity).

To avoid this, advances in vector engineering (such as capsid engineering, miRNA-regulated expression cassettes, etc) and delivery techniques (such as immune suppression, administration to immune privileged sites, among others) are being developed.

Specificity in the cell entrance

The ideal way of getting to a cell will be the one most of viruses do, *via* receptor-mediated endocytosis (Blaas, 2016; Cossart & Helenius, 2014). This process starts with a contact between a viral structure and a receptor localized on the surface of the targeted cell. Different viruses, once they contact with the cell in an extreme of fillopodia, are slided to the cell surface (Lehmann *et al*, 2005; Mercer *et al*,

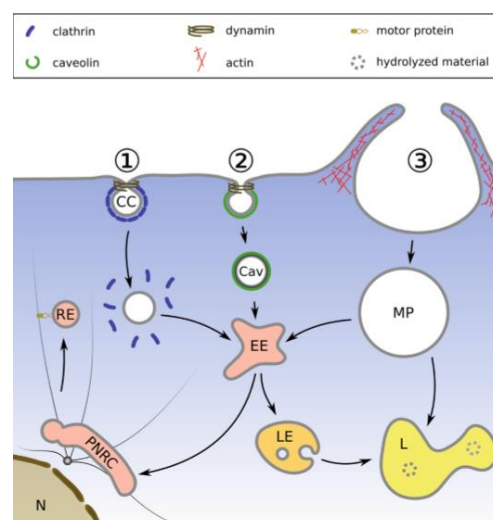


Figure 21. Diagram of the major mechanism of cell entry by viruses. (1) Clathrin mediated endocytosis, (2) caveolar endocytosis, and (3) pinocytosis. (Blaas, *et al*, 2016)

2010). Protein-receptor contact activates different signaling cascades that leads to the internalization of the virus. This process is a specific one, due to requirement of viral protein and the receptor.

Delivery of the cargo

Most of viruses, once they are endocytosed into the cell, enter the endosome-lysosome route (as shown in the fig. 2I). Once they are internalized, endocytic vesicles are formed. Different vesicles with acid hydrolases, coming from the Golgi are fused, forming the early endosomes. This process of adding different acidic vesicles will continue till the formation of the late endosomes and lysosomes. During this process the pH of the vesicle will gradually decrease (Luzio *et al*, 2000). This low-pH and the enzymatic environment trigger a conformational change of the viral proteins, as it happens with the rabies virus (Ross *et al*, 2008). These changes trigger membrane fusion and the release of the viral particle into de cytosol.

NANOMEDICINE

Taking into account that none of the systems above fulfill all the requirements, recent advances in nanotechnology may help us find the solution.

Carbon nanotubes (CNT) have the intrinsic ability of recruiting the surrounding proteins on their surfaces through non-covalent interactions adopting different biomimetic identities. This protein functionalization provides carbon nanotubes with different “biological camouflages” that are critical for instance, in their receptor mediated energy-dependent endocytic uptake (Lacerda *et al*, 2012)). Functionalized carbon nanotubes thus, are promising materials for the development of intracellular delivery tools because they also have the capacity to escape from the endo-lysosomal compartment after endocytosis (Al-Jamal *et al*, 2011; Mu, 2009).

In the view of all this, in this study, we have used sub-micrometric solid silica (SiO₂) particles with a carbon nanotube corona, a key element responsible for the carrier performance. The high aspect ratio and surface reactivity of carbon nanotube provides these new engineered carrier systems with an extraordinary surface area where to attach ligands for targeted cell delivery. The solid silica sphere will be used as a proof-of-concept, and can be substituted in the future for empty capsules or nanomaterials with biological properties.

2. Objectives

The long-term objective of this project will be the design of a “magic bullet” that will be able to target specifically any type of cell with any type of therapy. To achieve this aim, we have characterised the bio-synthetic interaction of silica solid spheres (500 nm) coated with carbon nanotubes synthesised at the University of Vigo with human cultured cells.

Thus, the goals of this work are;

- i) To study the toxicity of these particles in HeLa cells,
- ii) Investigate the entry mechanism,
- iii) Identify the intracellular localization and
- iv) Demonstrate particle carbon nanotubes loaded molecules release.

3. Material and Methods

3.1 HeLa Cell Culture

HeLa cells (immortalized human cervical cancer cell line) were maintained at 37°C and 5% CO₂ in EMEM (Eagle's Minimum Essential Medium) supplemented with 10% fetal bovine serum (FBS), gentamicin 1:1000 (from Gibco) and were subcultured by treatment with trypsin-EDTA at 90% confluency.

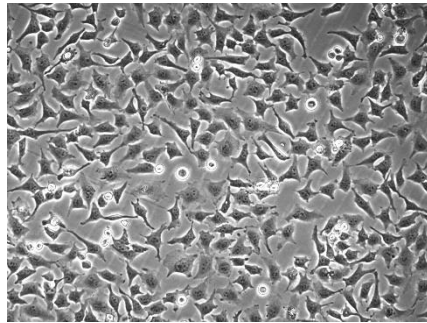


Figure 1M: photograph of HeLa culture in EMEM supplemented with 10% FBS and Gentamicin

3.2 Particles

The carbon nanotube coated particles were designed reproducing the morphology of typical eukaryotic viruses, often round shapes displaying spicules on their surface that serve as ligands for receptor mediated endocytosis (Fig. 2-A). As it is mentioned before, these structures have a 500 nm solid silica cores and a carbon nanotube corona. (Fig. 2-A). As a proof of concept to demonstrate CNT-molecule delivery, a dye (5-TAMRA) was linked to the silica spheres.

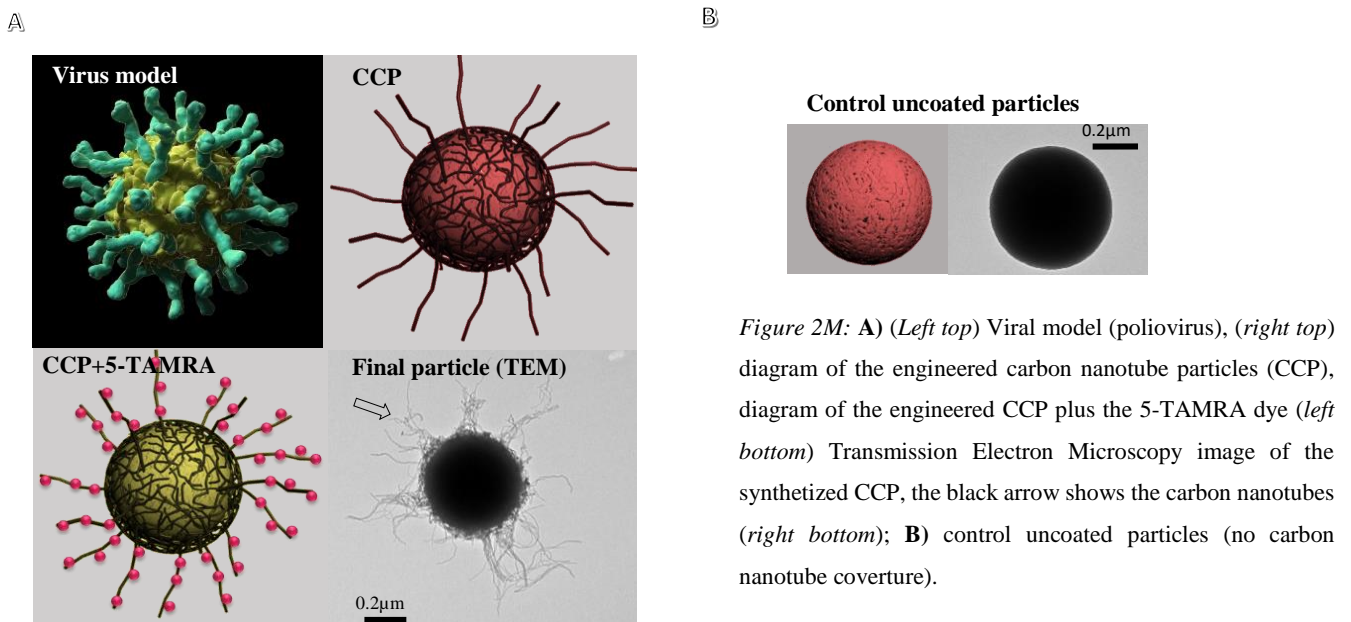


Figure 2M: **A**) (Left top) Viral model (poliovirus), (right top) diagram of the engineered carbon nanotube particles (CCP), diagram of the engineered CCP plus the 5-TAMRA dye (left bottom) Transmission Electron Microscopy image of the synthesized CCP, the black arrow shows the carbon nanotubes (right bottom); **B**) control uncoated particles (no carbon nanotube coverage).

3.3 Functionalization of the particles

Particles were first washed with PBS by centrifugation and then functionalized with a suspension medium based on 30% FBS + EMEM, plus mild sonication of 3 cycles of 2 seconds each pulse at a frequency of 20 kHz in a SONICS Vibracell VCX130, before the addition to the cells.

3.4 Toxicity of particles

Cells have mainly two different ways to die; **necrosis** (cell membrane rupture) and **apoptosis** (programmed death). To study the *necrotic cells* a trypan blue assay was performed. The trypan blue is able to enter cells that have a permeabilised cell membrane, typical in necrotic cells. Quantification of the cell survival was calculated in a hemocytometer, trypsinizing the culture, centrifuging it at 1200 r.p.m. during 2 minutes and resuspending it in a mix of trypan blue + EMEM (1:1 dilution) 1mL. The number of cells counted in the chamber was used to calculate the concentration of alive cells in the mixture.

$$[\text{Cell}] = \left(\frac{\text{n}^\circ \text{ of cell counted}}{(\text{proportion of chamber counted})(\text{volume of squares counted})} \right) \left(\frac{\text{Volume of diluted sample}}{\text{original volume mixture in sample}} \right)$$

To study the *apoptotic cell death* and to analyse possible cell cycle changes we employed flow cytometry. Once HeLa cells were incubated with the particles, they were detached with trypsin, washed with HBSS and centrifuged at 1000rpm during 10 minutes. Once the supernatant is taken out paraformaldehyde at 4% is added to fix those cells during 15 minutes and then it is removed centrifuging the sample at 1000rpm during 10 minutes. Next, permeabilization is performed by adding PBST 1% during 15 minutes. After this step, cells are counted to be sure that in all the different samples the same number of cells are used, and later they are dyed with a mixture of Hoetsch (1:1000) and PBST 1%..

3.5 Cellular uptake of the particles

Cellular uptake of CCPs and control uncoated particles were calculated. Functionalized particles were added to two 60mm petri dishes containing HeLa cells on cover slips. After the addition of particles, the cover slips were thoroughly washed with medium (EMEM) at different times; 15', 30', 60', 120' and overnight (o/n), and were fixed with 4% of paraformaldehyde (16% Solution, EM Grade; Electron Microscopy Sciences, PBS 1X, DW).

3.6 Staining and Confocal Microscopy Imaging

3.5.1 Staining

Once fixing is finished and after washing the cells with PBST 0,1%, permeabilization of the membrane with triton 1% during five minutes is needed.

After this step and the consecutive three washes with PBST 0,1%, staining was proceeded. Phalloidin-tetramethylrhodamine B isothiocyanate and Hoechst dye (Bisbenzimidazole) (both from Sigma-Aldrich) were

used to stain actin and DNA. Acridine orange (Sigma-Aldrich) or LysoTracker® Deep Red (Thermo Fisher) were used to stain endosomes-lysosomes. Phalloidin (1:2000) was incubated for 45 minutes whereas Hoechst (1:4000) was done for 10 minutes. All of them were washed with PBST 0,1%.

Slips are now prepared to put them on slides to later observe them at the microscope.

3.5.2 Confocal Microscopy

In a conventional fluorescence microscope although you can obtain high resolution images and high contrast, it has a focus problem because it has both, in-focus and out-of-focus light. On the contrary, a confocal microscopy uses point illumination and a pinhole in an optically conjugate plane in front of the detector to eliminate out-of-focus signal so that the optical resolution is much better. The confocal microscopy images used in this work were obtained with a Nikon A1R confocal microscope and processed with the NIS-Elements Advanced Research software. For quantification, cell images were taken with the 20x lens was used with an open pinhole.

Live cell observation was performed using acridine orange (1:2000) (Sigma-Aldrich) or LysoTracker® Deep Red (1:10) (Thermo Fisher). Both probes stain acidic compartments such as lysosomes where they are sequestered producing a green/red emission when excited with blue/red light respectively. Acridine Orange is a metachromatic fluorophore and a lysosomotropic base ($pK_a = 10.3$) which diffuses into cells and accumulates in lysosomes by proton trapping. This accumulation produces a change in the fluorescence emission of the probe (from cytosolic green to red within the lysosomes due to concentration-dependent stacking of the acridine orange). The cells were incubated with the particles (final concentration of 10 $\mu\text{g/ml}$), stained *in vivo* for 60 min at 37°C, and rinsed with DMEM (Dulbecco's Modified Eagle Medium) before live high-resolution confocal imaging. This was performed by confocal microscopy using a Plan Apochromatic 100x oil N.A. 1.49 objective.

3.5.3 Transmission electron microscopy (TEM)

TEM was also used to localize cytoplasmic CCP. Pelleted HeLa cells were fixed with 1% glutaraldehyde in 0.12 M phosphate buffer, washed in 0.12 M phosphate buffer, post-fixed in 1% buffered osmium tetroxide, dehydrated in a graded acetone series, embedded in Araldite, and stained with lead citrate-uranyl acetate. Araldite sections (ca. 70 nm) were observed using a transmission electron microscope (JEOL JEM 1011).

3.7 Quantification of particles

For each different time and experiment 5 photographs were randomly taken with a dry lens (20x). Digitalized images were edited with ImageJ 1.48v program. After splitting the channels in colours, nucleus and particles were counted making a threshold adjust (Fig 3 A). The nuclei were analysed with a size (pixel²) from 250 to infinite (Fig 3 B) and the particles from 0 to 10. The number of particles inside cells was calculated before quantifying the amount of particles outside the cells. For each experiment three replicates were done at different times.

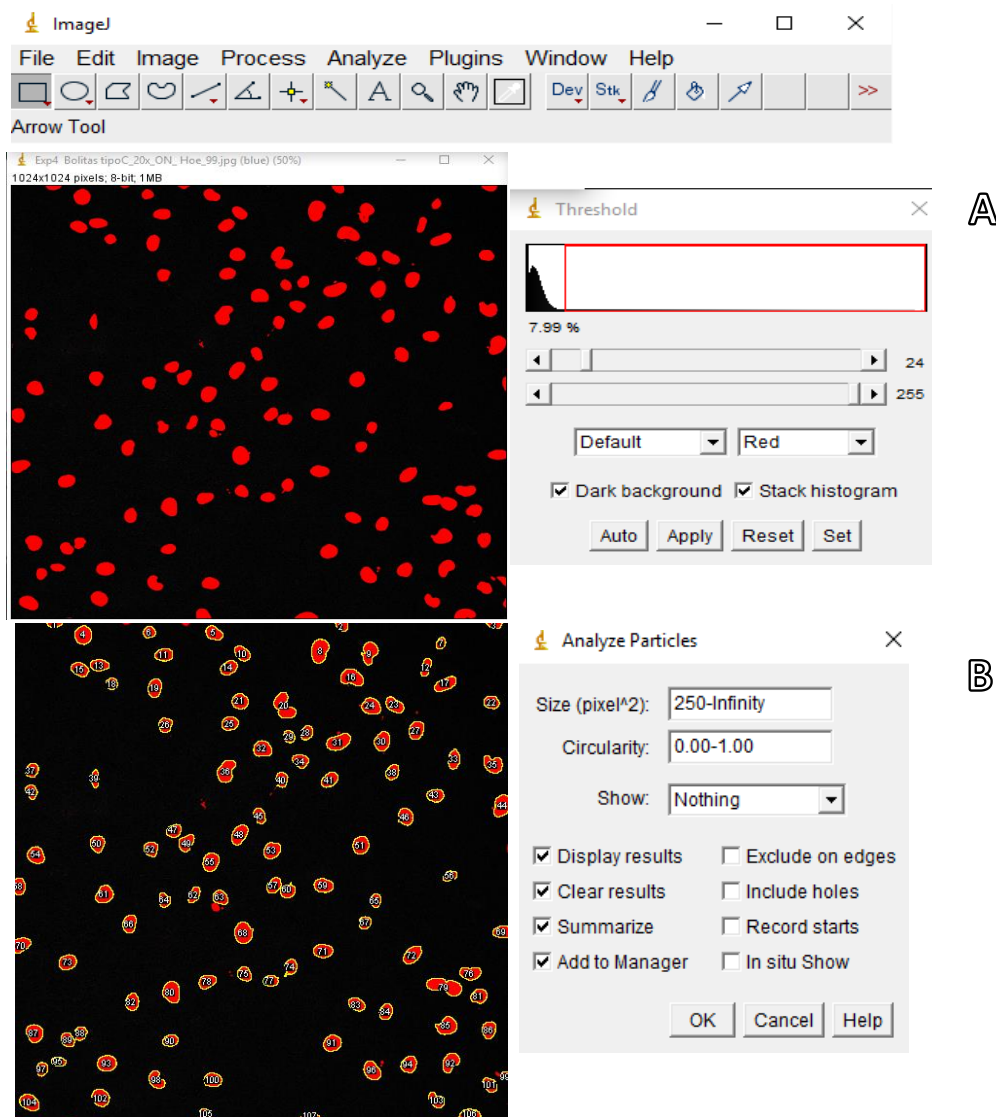


Figure 3M: Example of the quantification of the nuclei after the separation of the colour channels. A) the threshold adjusts and B) the particle analysis

3.8 Statistical analysis

A *t*-test statistical analysis was carried out to evaluate the significance of these results. Graphs and *t*-test analysis were done with standard commercial software. Quantitative results are expressed as mean values and standard error bars.

4. Results

4.1 Carbon nanotube coated particles do not trigger cytotoxic effects on HeLa cells

To evaluate the cytotoxic effect of the CCP we quantified cell death by necrosis (trypan blue assay) and apoptosis (flow cytometry). As the carbon nanotubes display a stabilization of the microtubules, arresting cells in mitosis, we analysed the cell cycle by flow cytometry focusing on the G₂ phase. HeLa cells were exposed to different concentrations of the two particles and we analysed particles with no exposure. As it is shown in the figure 1R no significant differences are observed in the percentage of necrotic (left image) either apoptotic cells (right image). Moreover, there were no changes in the different phases of the cell cycle (Fig. 2R)

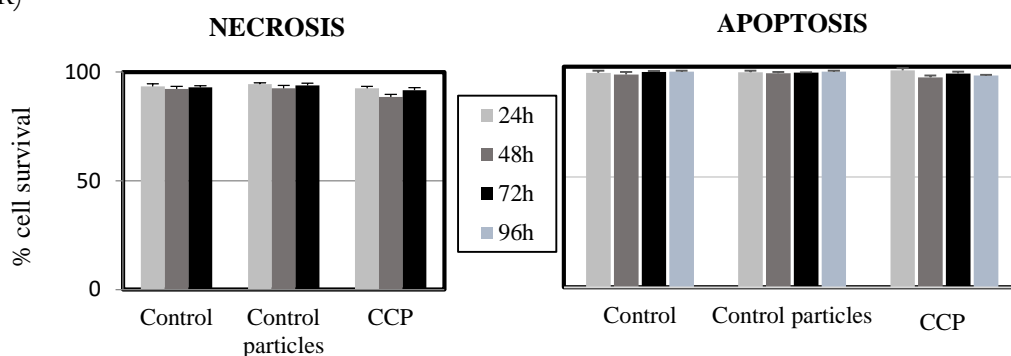


Figure 1R. (left) HeLa cells exposed to carbon nanotube coated particles do not display cell permeabilization typical of necrosis compared to controls. (right) Flow cytometry determination of apoptosis in control cells and cultures exposed to the carbon nanotube coated particles. These results correspond to 3 replicate experiments.

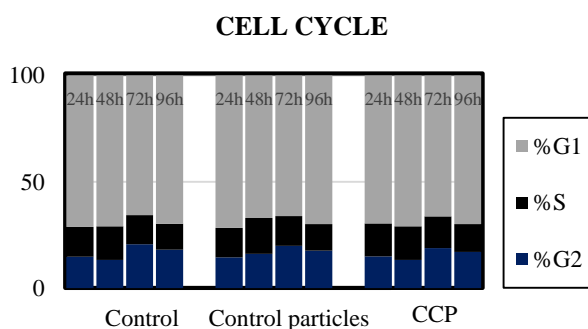


Figure 2R. Flow cytometric analysis of the cell cycle in control cultures and HeLa cells exposed to carbon nanotube coated particles at 24/48/72 and 96 h.

4.2 Carbon nanotubes enhance carbon nanotube coated particles entry

Once it is shown that these particles are not cytotoxic, we wanted to determine the entry mechanism. Using *time-lapse* video microscopy, we were able to determine that these CCP moved along the filopodia of the HeLa cells as it is shown in the figure 3R. This lateral particle movement has been previously described for viruses and it is called “viral surfing”. The particles are captured in the

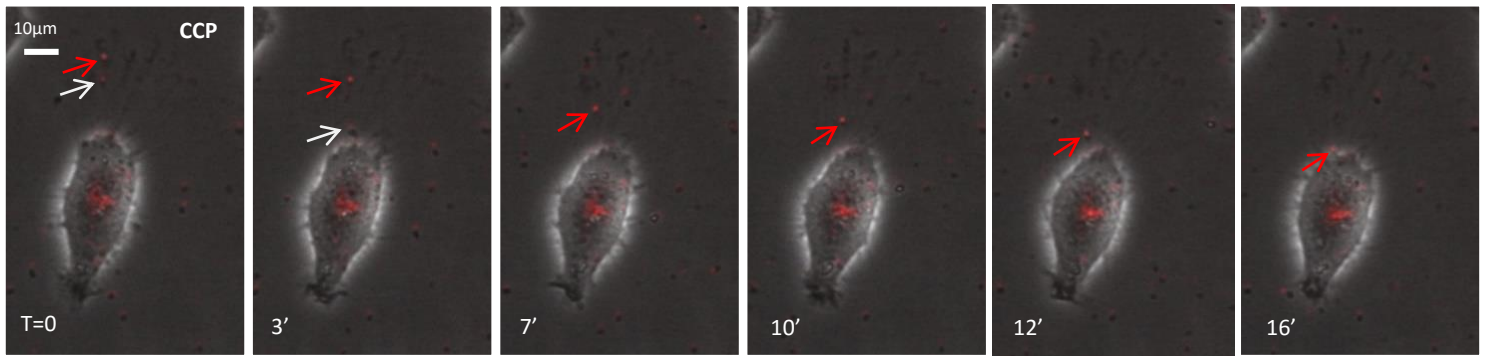


Figure 3R. Carbon nanotube coated particles do “viral surfing”. Time-lapse video microscopy frames of a live HeLa cell right after the administration of the TRIC- carbon nanotube coated particles. Red arrows mark how the particles is surfing along the filopodia of the cell.

extreme of the filopodia, presumably contact with cell receptors, and then are carried towards the cell body displaying this “viral surfing”. The red and white arrows in the figure 3R indicate two particles during this process. This phenomenon was not identified in the same experiments using control particles, suggesting uncoated particles have a different entry mechanism.

The fact that these two particles have a different entry mechanism can be corroborated with particle quantification after different exposure time. In the figure 4R we can observe the percentage of particles inside HeLa cells after 15, 30, 60 and 120 min of the administration. The percentages are calculated taking as the 100% the total overnight intracellular particle load. Thereby, it is shown that the carbon nanotubes coated particles enter faster and in a higher concentration than the control ones: for instance, after 15 minutes, almost the 10% of the particles are inside cells in the CCP, while less than a 3,5% are in the control particles. The quantification of the particles was done in confocal

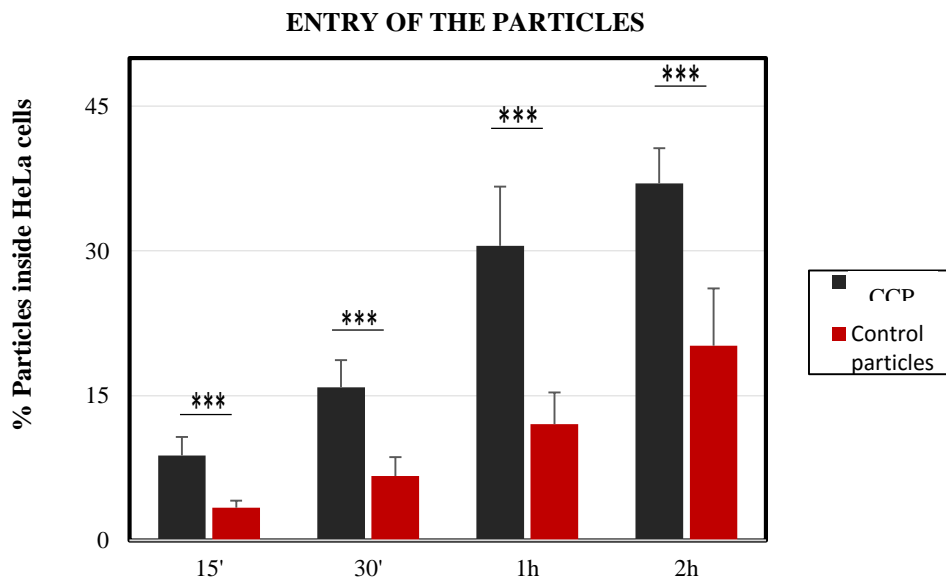


Figure 4R. Percentage of the different particles after 15 min, 30 min, 1 h and 2 h of exposure. These percentages have been calculated taking as a 100% the total overnight intracellular particle load for each

A1R microscope at low resolution with a 20x objective and a complete open pinhole, so that all the particles inside the cells were taken.

To illustrate these data single plane high resolution confocal microscopy images are shown after 30 minutes of exposure (Figure 5R). White arrows point out cells that have particles inside them, and as it is shown, more cells have carbon nanotubes coated particles, indicating a more efficient particle internalization.

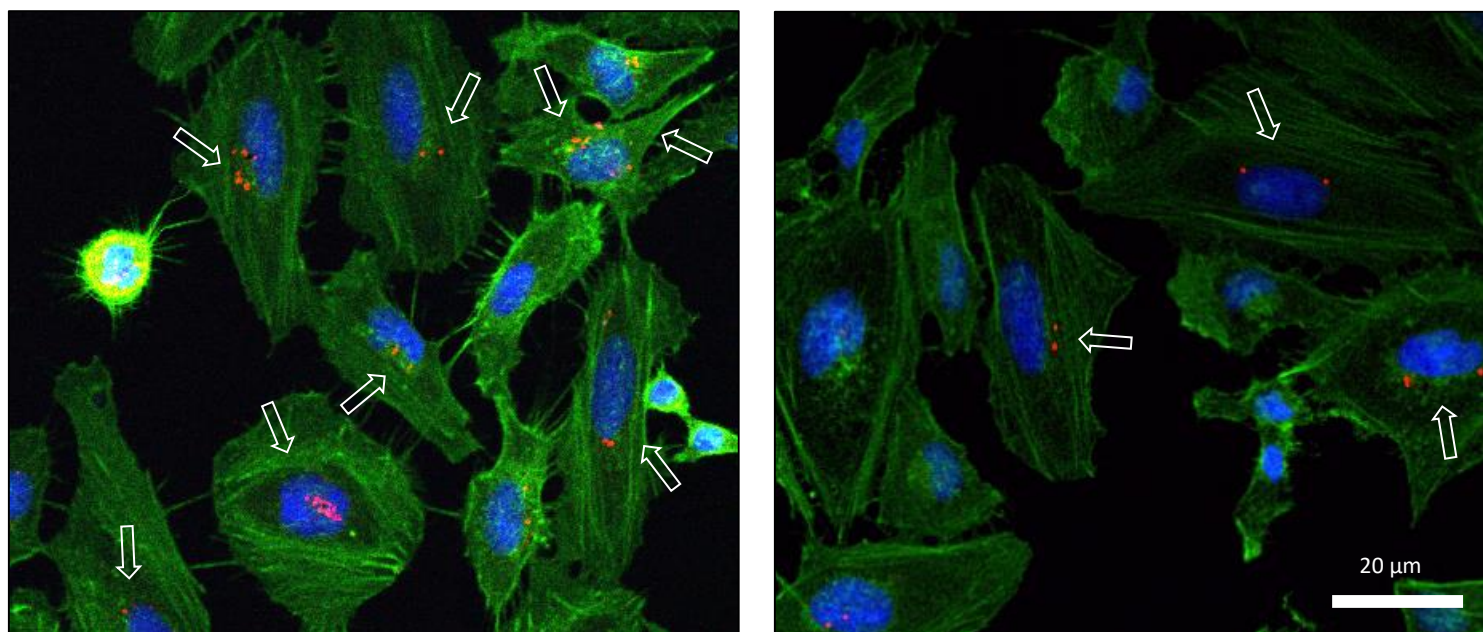


Figure 5R. Confocal microscopy image of HeLa fixed (4%) cells after 30' of exposure of (left) carbon nanotube coated particles and (right) silica particles. White arrows point out particles inside cells.

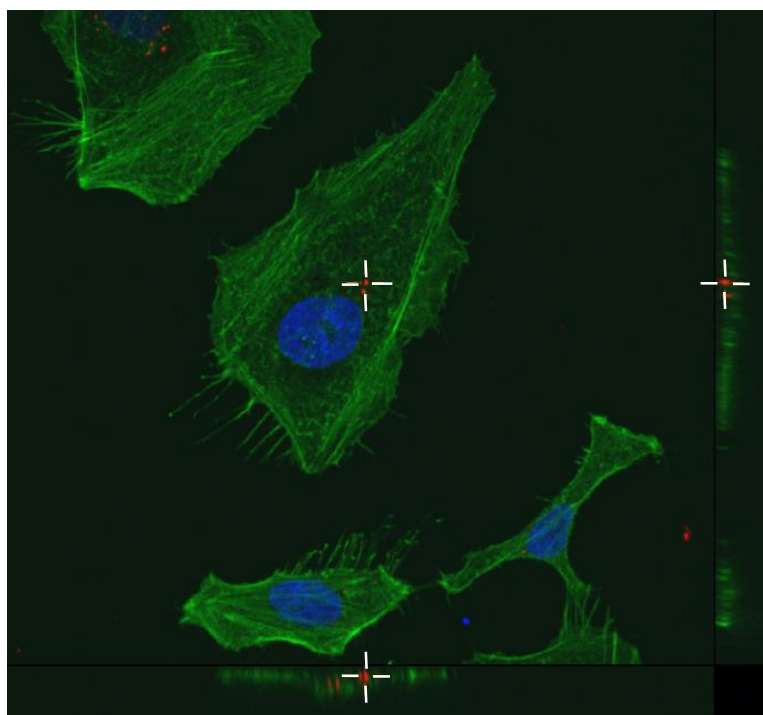


Figure 6R. Single plane confocal microscopy image of a carbon nanotube coated particles out of a Z-series. Lateral cellular Z projections demonstrating the localization of a single particle (in the white cross). The carbon nanotube coated particles can be unequivocally localized inside the cell after an overnight of exposure (actin in green channel; DNA blue channel).

Figure 6R shows a confocal microscopy image out of a Z-series. In the lateral projection images it is observable with no doubt how the carbon nanotube coated particle is localized inside the cell after an overnight.

4.3. Control uncoated particles are exocytosed after following the endo-lysosomes route.

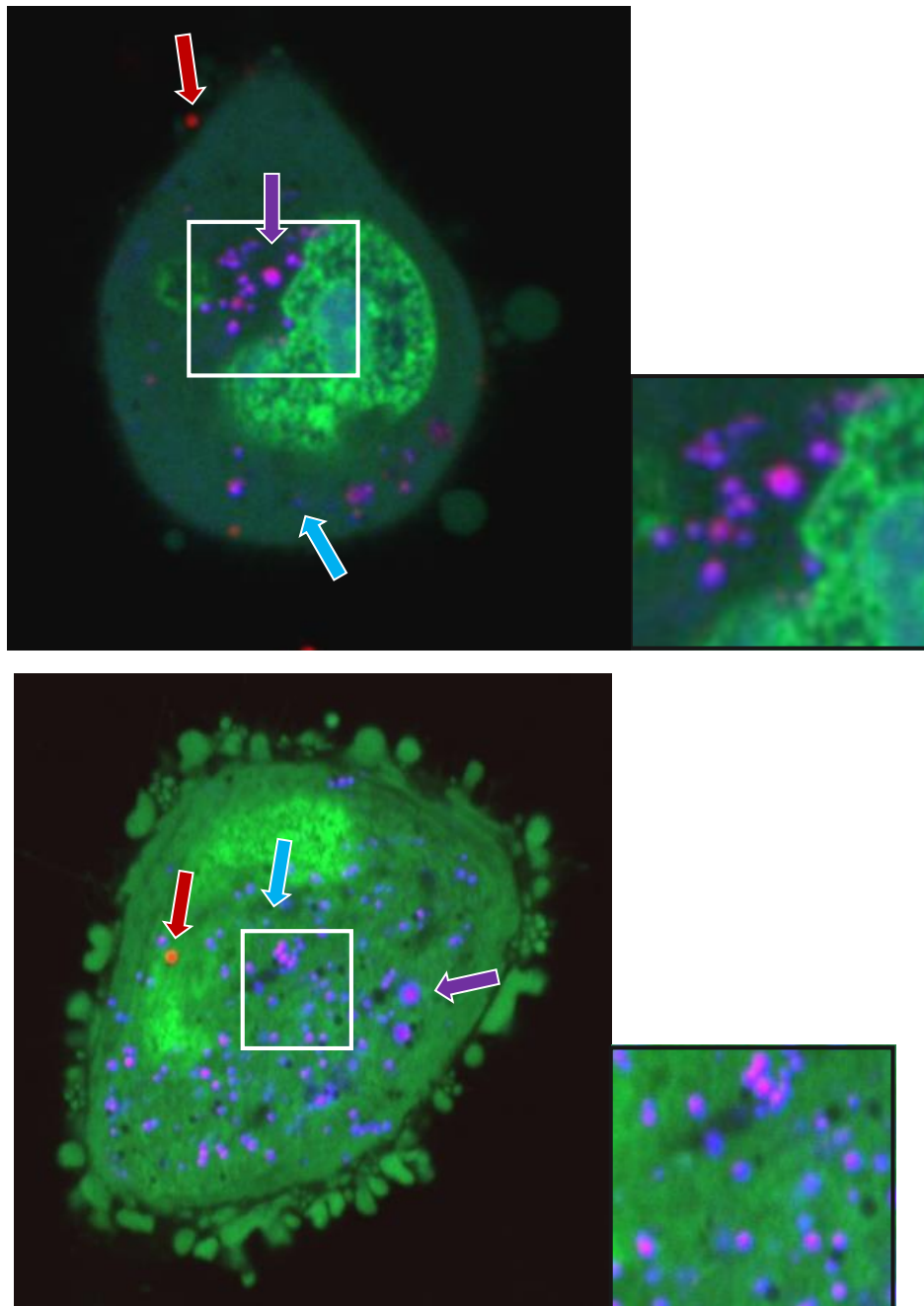


Figure 7R. Single plane confocal microscopy image of a live HeLa cell 2 h after the administration of carbon nanotube coated particles (*above*) and control g control particles (*below*) (red arrows). The cell was stained with Acridine Orange (green), and the lysosomes with LysoTracker (blue arrow). The lysosomes where carbon nanotube coated particles are, are pointed out with the purple arrow.

Taking into account that the internalization of these particles is not the same, we focused then on the intracellular trafficking and final localization. After the uptake of the particles the endosomal-lysosomal route was proposed. To confirm this entry route we stained live HeLa cells with two endo-lysosomal markers, acridine Orange and Lysotracker®. Figure 7R shows how after 2 h of exposure, both particles (7R-above CCP and -below control uncoated particles) are inside acidic vesicles as lysosomes.

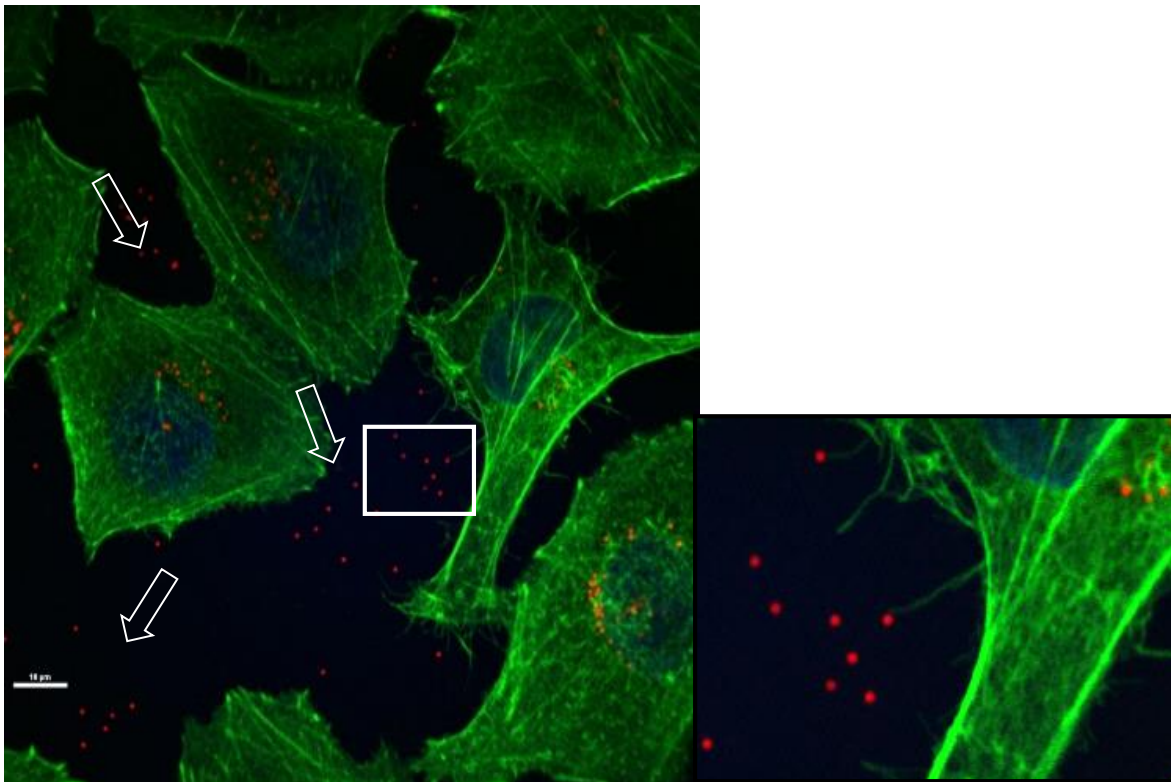
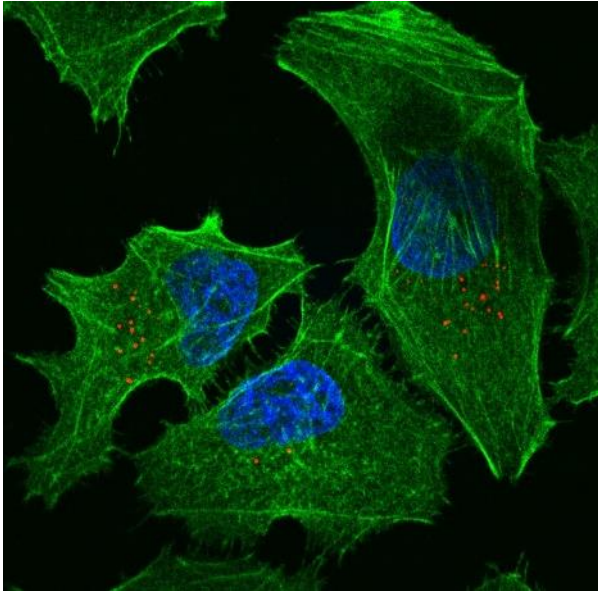


Figure 8R. carbon nanotube coated particles (*above*) and control uncoated particles (*below*) after an overnight of exposure. Cells were stained with Hoestch (1:4000) and Phalloidine 647 (1:1000) after been fixed with PF 4%. The white arrows point out control particles outside cells.

Intracellular *vs* extracellular quantification of particles revealed a higher number of control uncoated particles outside cells, suggesting active endocytic take up, followed by exocytosis (Figure 8R).

We thoroughly washed the cells after 15, 30, 60, 120 min and overnight of the administration of the particles (control and CCP), quantifying the extracellular ones. Approximately 1/3 of the total (extra+intracellular) particles were extracellular after 2h and an overnight of exposure as it is shown in the figure 9R. Endocytosis-exocytosis cycles were seen when doing the quantification of particles after an overnight (t=0) and later times (30, 60, 120 min, 3h, 4h, 6h and O/N; Figure 10R).

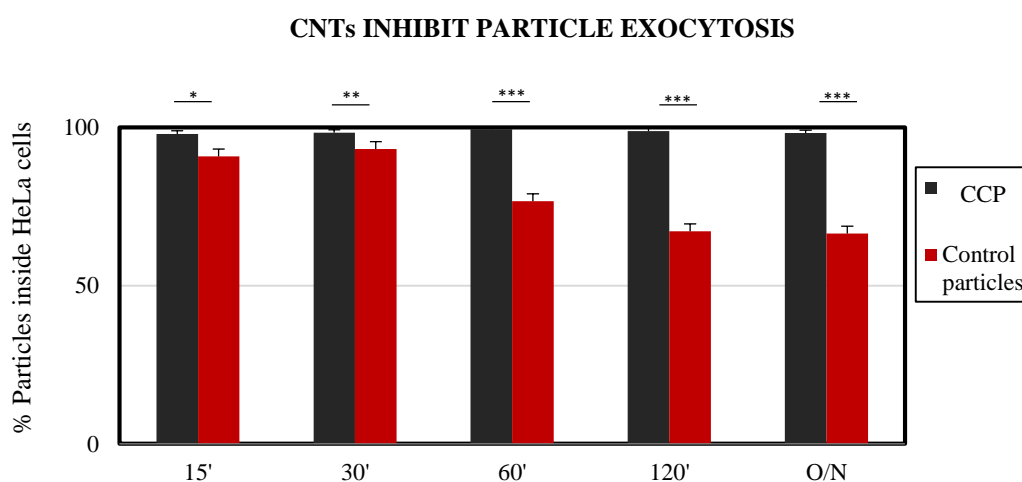


Figure 9R. Percentage of particles within HeLa cells is shown after 15, 30, 60, 120 min and an overnight of exposure, compared to the total particles (inside and outside cells) in each image.

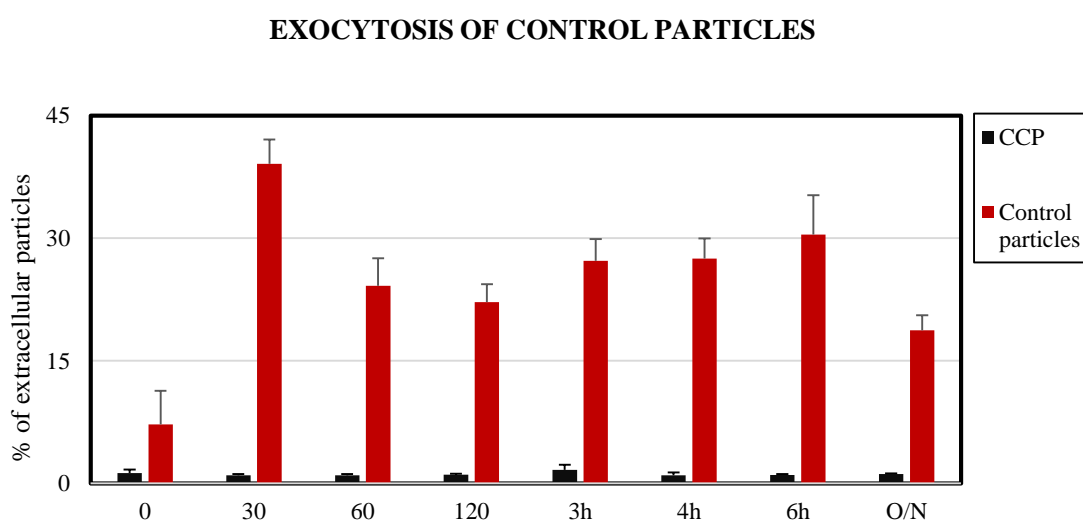


Figure 10R. Quantification of the extracellular particles in HeLa cells at different times of exposure (T0=overnight) taking as he 100% the particles outside and inside cells.

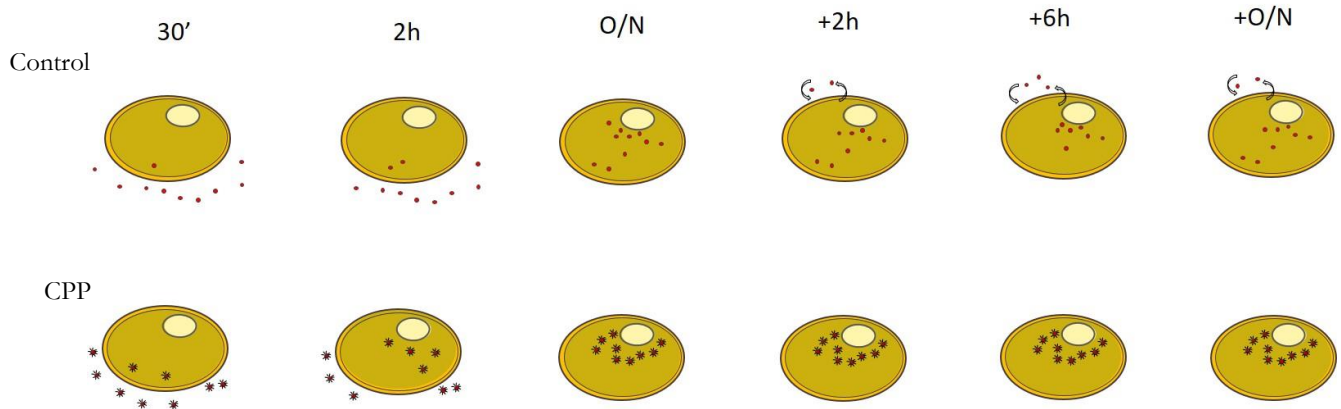


Figure 11R: representation of the endocytosis-exocytosis cycle at different times after exposure to the control uncoated particles (*top*) and the CPP (*bottom*); 30 min, 2 h, O/N, 14 h, 18 h and 24 h.

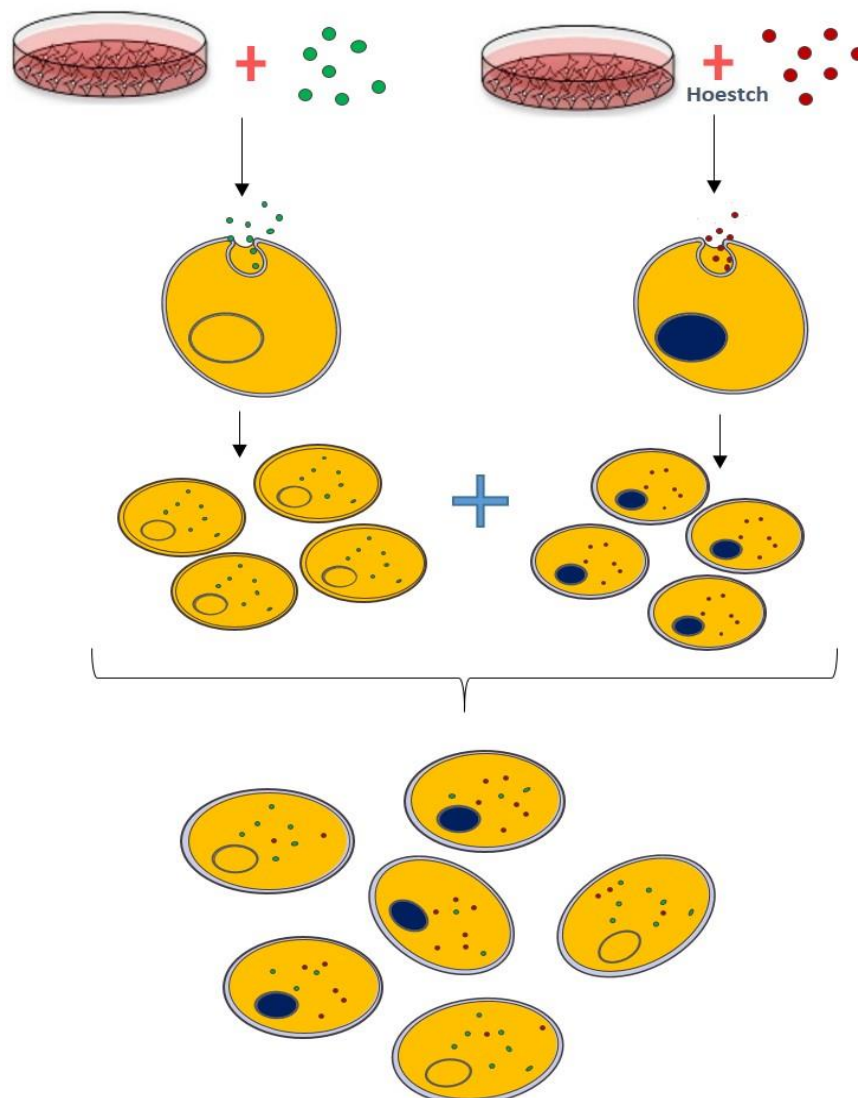


Figure 12R: representation of the co-culture with HeLa cell after the exposure of the control particles in red (rhodamine) and in green (fluorescein).

To investigate the endocytosis-exocytosis cycle we performed two different experiments. We first co-cultured two separate cultures of HeLa cells with the control uncoated particles, either coloured in

red (rhodamine) or in green (fluorescein), see figure 12R. The co-culture lasted 24h and then confocal microscopy was performed. As we can see in the figure 13R (above) HeLa cells display intracellular particles of both colours, suggesting the exocytosis and later endocytosis process. The second experiment consisted on co-culturing green-stained HeLa cell (cell green) devoid of particles with unstained cells plus red control uncoated particles. As figure 13R (bellow) demonstrates, green control uncoated particles have been able to exit from the cells and be endocytosed for other cells nearby.

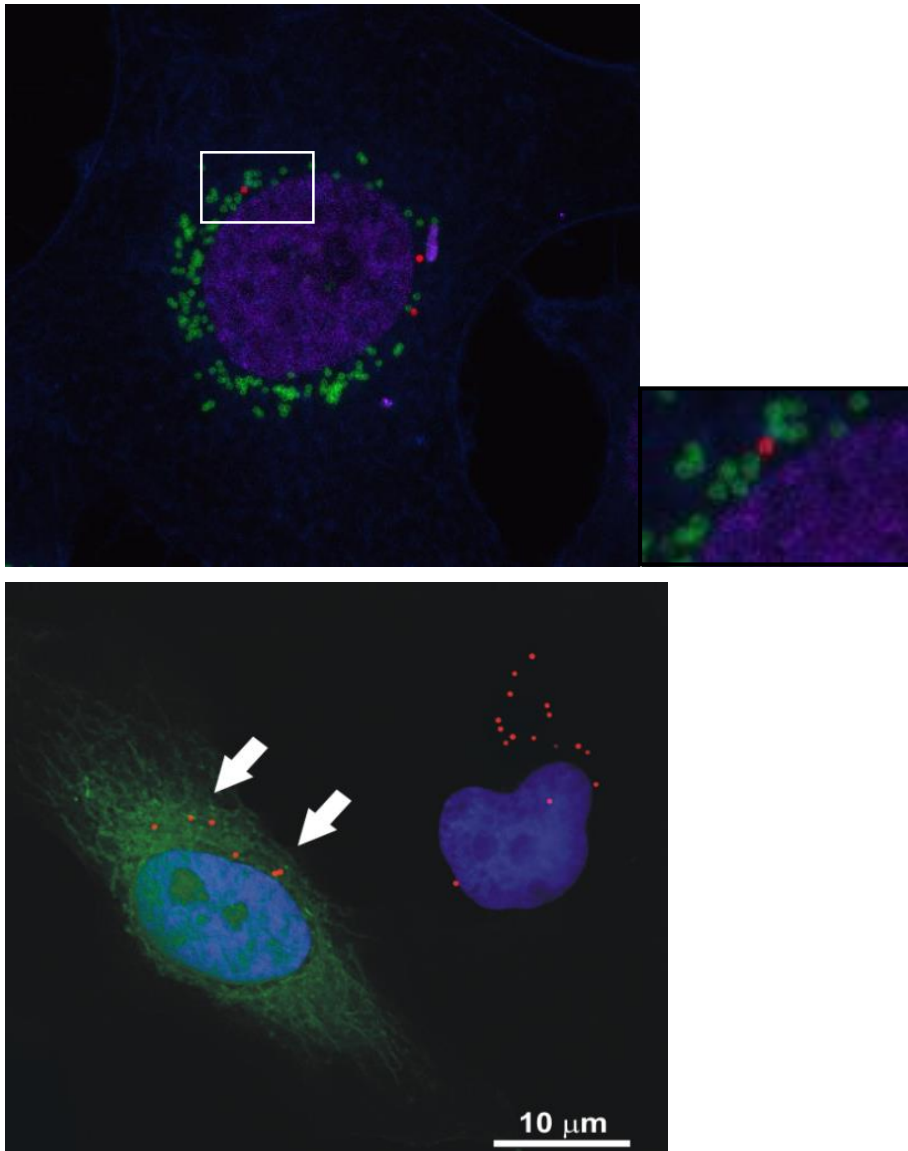


Figure 13R: (above) Single Z-plane confocal microscopy image of HeLa cell containing originally only control particles coloured in green and now displaying red ones captured from the surrounding nearby cells, first experiment. (below) Single Z-plane confocal microscopy image of two cells. A green stained HeLa cell originally with no particles, and an originally unstained HeLa cell plus red control particles. Nuclei are labelled in blue.

4.4. Carbon nanotube coated particles escape the endo-lysosomal compartment into the cytoplasm

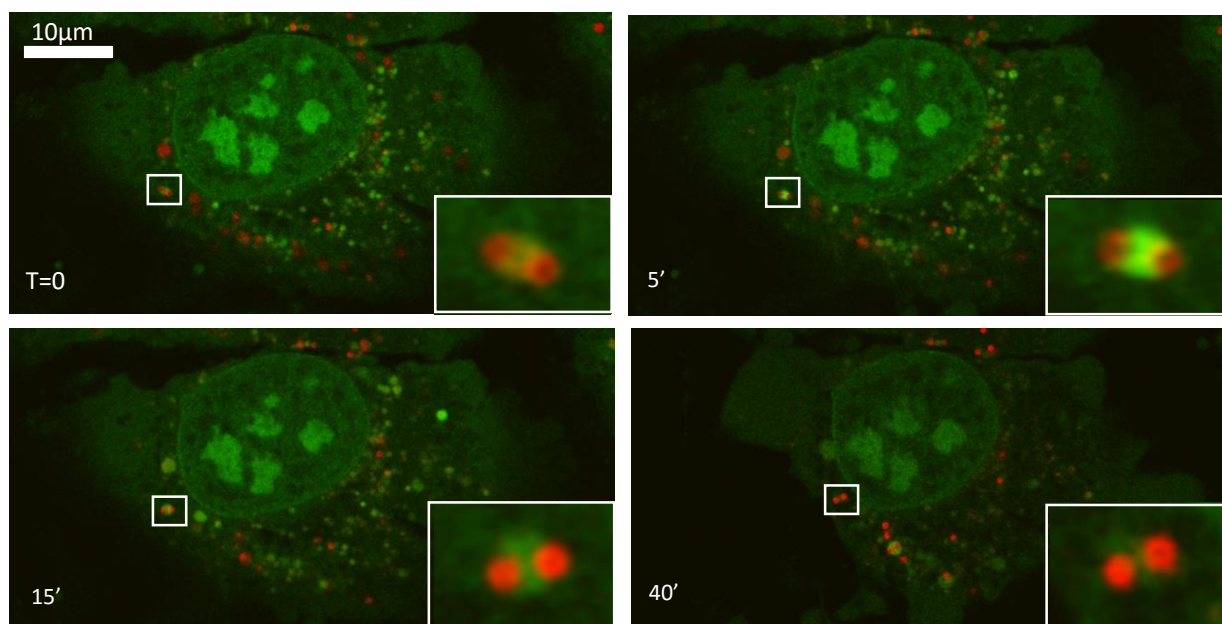


Figure 14R. Time-lapse confocal video microscopy of CCPs inside a HeLa. Single Z-plain images of live HeLa cells stained with Acridine Orange (1:2000) (green) 48h after CCP exposure. Two CCPs (red) escape from a lysosome.

To investigate the intracellular destiny of the CCP we first employed high resolution confocal video-microscopy on live stained cells. As it is observed in the video photograms shown in figure 14R, two

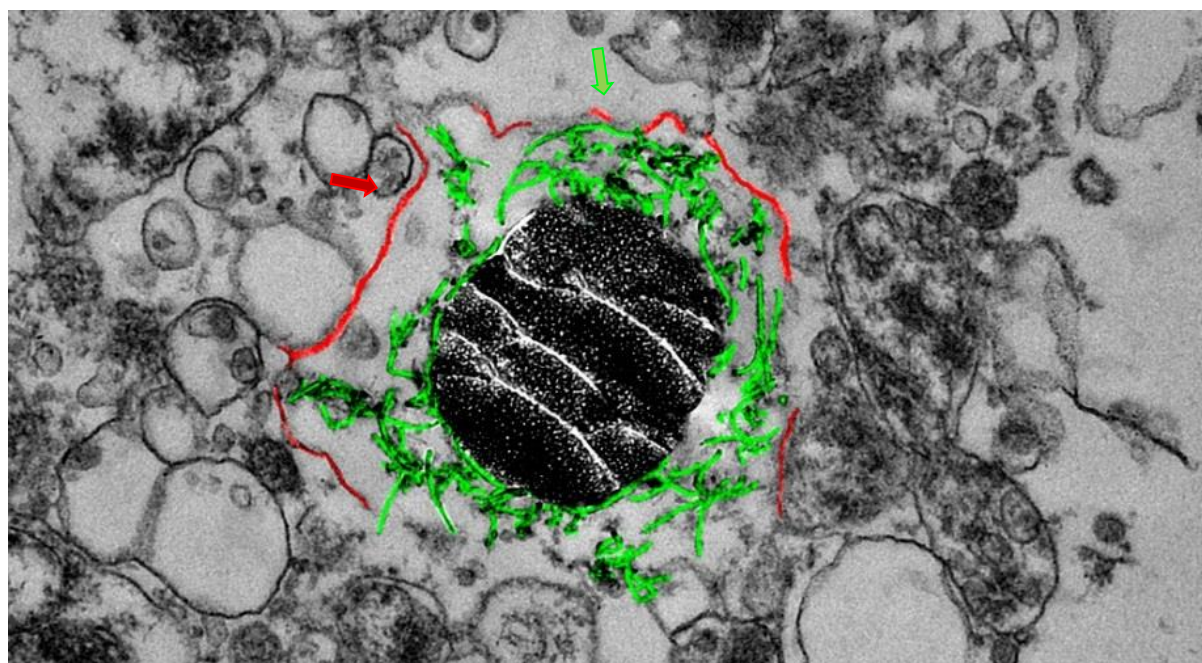


Figure 15R. Transmission Electron microscopy section of a HeLa cell cytoplasm displaying a CNT-coated particle (black arrow) escaping from the lysosomal membranes (red arrow). Carbon nanotubes (green arrow) tear apart the lysosomal vesicle favouring CNT-coated particle escape to the cytosol.

carbon nanotube coated particles escape simultaneously from an endosome labelled in green with acridine orange. This phenomenon was not observed with the control particles, suggesting that the carbon nanotubes are responsible for the exit. To confirm this results we performed transmission electron microscopy with ultrafine sections of HeLa cells plus CCP. As it is shown in the figure 15R, the lysosomal membrane (painted in red) has got ruptures due to the action of the carbon nanotubes (painted in green) attached to the particle.

4.5. Carbon nanotube coated particles release molecules linked to the carbon nanotubes

To demonstrate the functionality of the CCP surface for the intracellular therapeutic delivery, as well as to show further evidence of the early endosomal membrane rupture, we performed a proof-of-concept test where the surface of the nanotubes of the CCP were functionalised with a red fluorescent dye (5-TAMRA). As it is shown in the figure 16R the 5-TAMRA dye is present in the cytoplasm showing that the dye has been released from the carbon nanotubes after CCP exposure to the endosomal reducing environment. There is no observable cytoplasmic fluorescence for the control uncoated particles (fig. 15R *left*).

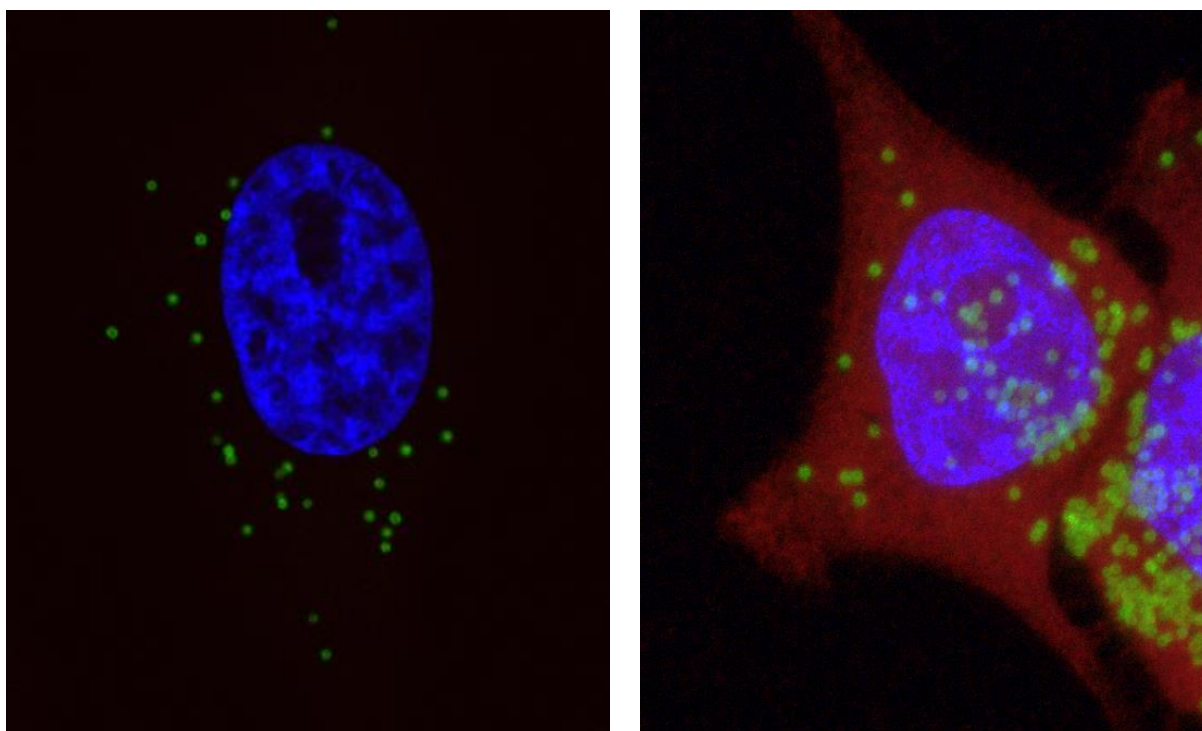


Figure 16R. Single Z-plane confocal microscopy image of HeLa cell after 24h of the administration of green uncoated control particles (*left*) and green CCP functionalised with 5-TAMRA dye (*right*).

5. Discussion

The fact that these CNT-coated particles are not toxic might be an advantage for the therapeutic delivery system function of them.

CNT (50µg/mL) themselves have a cytotoxic (García-Hevia *et al*, 2015), anti-proliferative (Garcia Hevia *et al*, 2016) and anti-migratory (Garcia Hevia *et al*, 2015) effects. Our data reveal that at the same concentration, or even higher than 50µg/mL, that these particles do not produce in HeLa cells an increase in the percentage of death cells or changes in the cell cycle. Control particles do not trigger any detectable cytotoxic effect either.

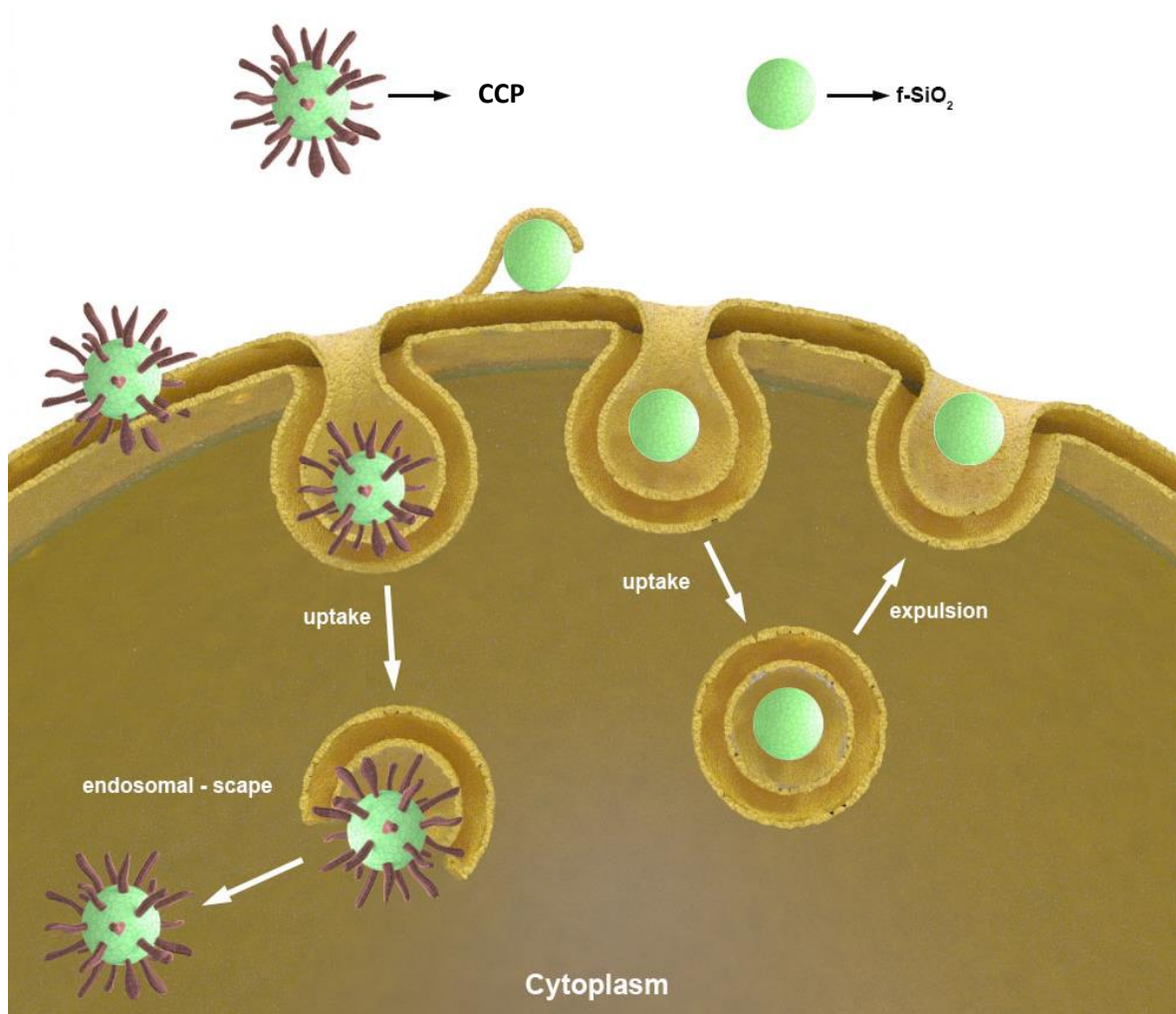
This no-cytotoxic effect might be due, on one hand to the binding of the carbon nanotubes to the particle surface. On the other hand, it is known that the size of silica nanoparticles (70 nm) might have effects on the metabolic cell activity of the cell (Al-Rawi *et al*, 2011) for instances increasing the amount of lactate dehydrogenase (LDH) and decreasing the metabolic activity when they are not functionalised with serum. In comparison, silica spheres of 200 and 500 nm had neither an effect on LDH release nor on the metabolic activity even when they are not functionalised. Yet, different studies have shown toxicity in different cell lines such as HaCaT (Yang *et al*, 2010) or human endothelial cells (Napierska *et al*, 2009). Thus, we would need further investigation on the cell lines to corroborate their cell viability of the CCPs.

Different mechanism of cell entry haven been proposed for nano- or sub-micron particles. In live organism such as bacteria, it is reported that the shape; rods, spirals or ellipsoids, has critical implications in cell recognition and can directly affect the endocytosis pattern (Young, 2006). As it happens with the live organism, the shape of different synthetic nano-vehicles is also important to determine the cellular uptake (Oh & Park, 2014). Therefore, we designed these particles with a round shape in order to mimic the morphology of live organisms such as many eukaryotic viruses. Focusing on the cell entry mechanism, it is remarkable that the carbon nanotube coated particles are able to mimic viruses. Functionalised particles are recruited by filopodia, and once they flow along these protrusions, enter into cells via receptor-mediated endocytosis. This kind of surfing phenomenon has been identified on viruses (Lehmann *et al*, 2005; Mercer & Helenius, 2008) and exosomes (Heusermann *et al*, 2016). As it has been shown in this study, control uncoated particles do not present this mechanism, suggesting that carbon nanotubes are actually the ones that cause this surfing. Indeed, functionalised carbon nanotubes themselves are actively captured by cells *via* receptor-mediated endocytosis (Lacerda *et al*, 2012).

Once CCP and control uncoated particles are internalised, both follow the endosome-lysosome route. Yet, as it is demonstrated in the results, control particles later are next exocytosed. The post-lysosomal exocytosis has been described for different nanoparticles (Oh & Park, 2014) including silica nanoparticles (Slowing *et al*, 2011). Although exocytosis of nanomaterials is still not fully understood, previous studies suggest that exocytosis implies lysosomal fusion to the cell membrane (Jahn & Sudhof, 1999). The fact that these control uncoated particles are exocytosed could be interesting from the point of view of transcytosis.

CCPs, however, escape the endosome-lysosome route as carbon nanotubes themselves do (Al-Jamal *et al.*, 2011). Once are inside the lysosome, the acidic environment and the low pH may degrade the proteins coating the carbon nanotubes. Since naked carbon nanotubes are apolar, they are likely to interact with the lysosomal membrane after protein degradation, tearing the vesicle apart and escaping into the cytosol. This lysosomal escape mechanism is similar to the one displayed by many enveloped viruses, showing again a mimic behaviour of these CCP. The removal of the BIOcorona of the carbon nanotubes was also proved with the experiment of the release of the 5-TAMRA. The dye release to the cytosol reveals carbon nanotube surface modifications and lysosomal membrane permeabilization or rupture.

Summarizing, as it is shown in the diagram below, CCPs behave in a unique viral biomimetic way compared to control uncoated particles. The carbon nanotube corona provides these particles with a more specific and faster way to trigger endocytosis and to enter in the endosome-lysosome route,



Representative scheme of the internalization mechanism proposed. The CCPs interact with the cell following virus-like mechanisms. After internalization CCPs are able to escape from the endo-lysosome (left). The uncoated control silica particles are also taken up under but are later exocytosed.

being able to escape from these membranes without causing cytotoxic effect and releasing carbon nanotube loaded cargo molecules (a dye in this case) to the cytosol.

The characteristics [i) do not produce a cytotoxic effect, ii) be able to mimic the entrance into the cells, iii) mimic the endosome-lysosome escape and iv) be able to release a dye to the cytosol] that carbon nanotube coated particles have, give them the ability to be in the future a good targeted delivery system. The fact that the carbon nanotube coated particles do not produce a cytotoxic effect and are able to first, mimic the entrance mechanism of some live organism such as viruses and the endosome-lysosomal escape, and second to release the dye to the cytosol, make of carbon nanotubes excellent Trojan –horse mechanisms to improve synthetic intracellular carrier systems for targeted cell delivery.

6. Conclusions

The ideal delivery system need to i) recognise specifically cells, ii) be able to escape the endo-lysosome route to the cytoplasmic delivery, iii) be able to deliver more than one type of molecules simultaneously such as proteins and nucleic acids and iv) do not trigger a cytotoxic effect.

The model proposed in this project (the CCP particle) is capable to:

- i) Not trigger a cytotoxic effect in HeLa cells with different concentration (until 100µg/mL) of the particles.
- ii) Enter to the cell via receptor-mediated endocytosis due to their functionalization with fetal bovine serum proteins such as albumin.
- iii) Once they are inside the cells, follow the endosome-lysosome route and are able to escape them. The apolar characteristic of the carbon nanotubes help the particle escape from them.
- iv) With the degradation of the functionalised proteins inside the endosome-lysosomes, molecules linked before the functionalization are able to escape to the cytoplasm without losing their function.
- v) Due to their big size, they might be able to transport combination of both proteins and nucleic acids. This point could be really important, taking into account that the new advances in gene editing technologies such as CRISPR-cas, need a targeted delivery system capable of transporting protein and nucleic acids complexes.

These particles might be capable for a targeted delivery in the future. As we have seen in this work they have a lot of potential and advantages. Nevertheless, more studies are needed such as;

- Use empty or porous spheres instead of the solid ones, to see if they could be used as “transfecting hosts”
- Bind specific proteins or ligands to the carbon nanotube surface for targeted delivery
- Inject CCP in animal models to test in vivo toxicity, immune response and try targeted delivery

7. Bibliography

- Al-Jamal KT, Nerl H, Müller KH, Ali-Boucetta H, Li S, Haynes PD, Jinschek JR, Prato M, Bianco A, Kostarelos K & Porter AE (2011) Cellular uptake mechanisms of functionalised multi-walled carbon nanotubes by 3D electron tomography imaging. *Nanoscale* **3**: 2627–2635
- Al-Rawi M, Diabaté S & Weiss C (2011) Uptake and intracellular localization of submicron and nano-sized SiO₂ particles in HeLa cells. *Arch. Toxicol.* **85**: 813–826
- Blaas D (2016) Viral entry pathways: the example of common cold viruses. *Wiener Medizinische Wochenschrift*: 211–226
- Cossart P & Helenius A (2014) Endocytosis of viruses and bacteria. *Cold Spring Harb. Perspect. Biol.* **6**
- García-Hevia L, Valiente R, Fernández-Luna JL, Flahaut E, Rodríguez-Fernández L, Villegas JC, González J, Fanarraga ML (2015) Inhibition of Cancer Cell Migration by Multiwalled Carbon Nanotubes. *Adv Healthc Mater* **5**: 1640-4
- García-Hevia L, Valiente R, González J, Terán H, Fernández-Luna JL, Villegas JC & Fanarraga ML (2015) Anti-Cancer Cytotoxic Effects of Multiwalled Carbon Nanotubes. *Curr. Pharm. Des.* **21**: 1920–29
- García-Hevia L, Villegas JC, Fernández F, Casafont Í, González J, Valiente R, Fanarraga ML (2016) Multiwalled Carbon Nanotubes Inhibit Tumor Progression in a Mouse Model. *Adv Healthc Mater.* **5**: 1080-7
- Heusermann W, Hean J, Trojer D, Steib E, von Bueren S, Graff-Meyer A, Genoud C, Martin K, Pizzato N, Voshol H, Morrissey D, EL Andaloussi S, Wood M & Meisner-Kober NC (2016) Exosomes surf on filopodia to enter cells at endocytic hot spots and shuttle within endosomes to scan the ER. *J. Cell Biol.* **213**: Final revised manuscript submitted
- Canton I and Battaglia G (2012) Endocytosis at the nanoscale. *Chem. Soc. Rev.* **41**: 2545–2561
- Jahn R & Sudhof T (1999) Membrane Fusion and Exocytosis. *Annu. Rev. Biochem.*: 777–810
- Kukowska-Latallo JF, Bielinska U, Johnson J, Spindler R, Tomalia D a & Baker JR (1996) Efficient transfer of genetic material into mammalian cells using Starburst polyamidoamine dendrimers. *Proc. Natl. Acad. Sci. U. S. A.* **93**: 4897–4902
- Lacerda L, Russier J, Pastorin G, Herrero MA, Venturelli E, Dumortier H, Al-Jamal KT, Prato M, Kostarelos K & Bianco A (2012) Translocation mechanisms of chemically functionalised carbon nanotubes across plasma membranes. *Biomaterials* **33**: 3334–3343
- Lehmann MJ, Sherer NM, Marks CB, Pypaert M & Mothes W (2005) Actin- and myosin-driven movement of viruses along filopodia precedes their entry into cells. *J. Cell Biol.* **170**: 317–325
- Luzio JP, Rous B a, Bright N a, Pryor PR, Mullock BM & Piper RC (2000) Lysosome-endosome fusion and lysosome biogenesis. *J. Cell Sci.* **9**: 1515–1524

- Mercer J & Helenius A (2008) Vaccinia virus uses macropinocytosis and apoptotic mimicry to enter host cells. *Science* **320**: 531–535
- Mercer J, Schelhaas M & Helenius A (2010) Virus Entry by Endocytosis. *Annu. Rev. Biochem.* **79**: 803–833
- Mu Q (2009) Endosomal leakage and nuclear translocation of multiwalled carbon nanotubes: developing a model for cell uptake. *Nano Lett.* **9**: 4370–4375
- Napierska D, Thomassen LCJ, Rabolli V, Lison D, Gonzalez L, Kirsch-Volders M, Martens JA & Hoet PH (2009) Size-dependent cytotoxicity of monodisperse silica nanoparticles in human endothelial cells. *Small* **5**: 846–53
- Oh N & Park JH (2014) Endocytosis and exocytosis of nanoparticles in mammalian cells. *Int. J. Nanomedicine* **9**: 51–63
- Ross BA, Favi CM & Vasquez VA (2008) Glicoproteína del virus rábico: Estructura, inmunogenicidad y rol en la patogenia. *Artículo Espec.* **25**: 5
- Seow Y & Wood MJ (2009) Biological Gene Delivery Vehicles: Beyond Viral Vectors. *Mol. Ther.* **17**: 767–777
- Slowing II, Vivero-Escoto JL, Zhao Y, Kandel K, Peeraphatdit C, Trewyn BG & Lin VSY (2011) Exocytosis of mesoporous silica nanoparticles from mammalian cells: From asymmetric cell-to-cell transfer to protein harvesting. *Small* **7**: 1526–1532
- Tang MX, Redemann CT & Szoka FC (1996) In vitro gene delivery by degraded polyamidoamine dendrimers. *Bioconjug. Chem.* **7**: 703–714
- Yang X, Liu J, He H, Zhou L, Gong C, Wang X, Yang L, Yuan J, Huang H, He L, Zhang B & Zhuang Z (2010) SiO₂ nanoparticles induce cytotoxicity and protein expression alteration in HaCaT cells. *Part. Fibre Toxicol.* **7**: 1
- Young KD (2006) The selective value of bacterial shape. *Microbiol. Mol. Biol. Rev.* **70**: 660–703
- Zachary C. Hartman, Daniel M. Appledorn and AA (2008) Adenovirus vector induced innate immune responses: impact upon efficacy and toxicity in gene therapy and vaccine applications. *Virus Res.* **132**: 1–14

} <http://www.wiley.com/legacy/wileychi/genmed/clinical/>

